Asian Journal of Pharmaceutical Sciences 16 (2021) 374–386

Available online at www.sciencedirect.com

ScienceDirect

journal homepage: www.elsevier.com/locate/AJPS

Original Research Paper

Innovative color jet 3D printing of levetiracetam personalized paediatric preparations

Zengming Wang[a], *Xiaolu Han*[a], *Ruxin Chen*[a,b], *Jingru Li*[a,c], *Jing Gao*[a], *Hui Zhang*[a], *Nan Liu*[a], *Xiang Gao*[a], *Aiping Zheng*[a,*]

[a] *Department of Pharmaceutics, Institute of Pharmacology and Toxicology of Academy of Military Medical Sciences, Beijing 100850, China*
[b] *College of Pharmaceutical Sciences, Key Laboratory of Pharmaceutical Quality Control of Hebei Province, Institute of Life Science and Green Development, Hebei University, Baoding 071002, China*
[c] *School of Pharmacy, Xuzhou Medical University, Xuzhou 221000, China*

ARTICLE INFO

Article history:
Received 8 November 2020
Revised 18 January 2021
Accepted 3 February 2021
Available online 1 March 2021

Keywords:
Color jet 3D printing
Paediatric preparations
Personalized administration
Medicine dosage model
Immediate release

ABSTRACT

3D printing is a promising technology used in the fabrication of complex oral dosage delivery pharmaceuticals. This study first reports an innovative color jet 3D printing (CJ-3DP) technology to produce colorful cartoon levetiracetam pediatric preparations with high accuracy and reproducibility. For this study, the ideal printing ink consisted of 40% (v/v) isopropanol aqueous solution containing 0.05% (w/w) polyvinylpyrrolidone and 4% (w/w) glycerin, which was satisfied with scale-up of the production. The external and internal spatial structures of the tablets were designed to control the appearance and release, and cartoon tablets with admirable appearances and immediate release characteristics were printed. The dosage model showed a good linear relationship between the model volume and the tablet strength ($r > 0.999$), which proved the potential of personalized administration. The surface roughness indicated that the appearance of the CJ-3DP tablets was significantly better than the first listed 3D printed drug (Spritam®). Moreover, the scanning electron microscopy and porosity results further showed that the tablets have a structure of loose interior and tight exterior, which could ensure good mechanical properties and rapid dispersion characteristics simultaneously. In conclusion, the innovative CJ-3DP technology can be used to fabricate personalized pediatric preparations for improved compliance. Due to the stable formulation and fabrication process, this technology has the potential in scale-up production.

1. Introduction

With the proposal of precision medicine, the demand for personalized medicine has dramatically increased, while traditional 'one-size-fits-all' treatment approaches are still prevailing in clinical [1–3]. Especially for pediatric preparations, a series of problems such as unavailability of appropriate dosage forms, deficiency of pediatric doses, palatability of pediatric dosage forms and difficulty in

* Corresponding author.
E-mail address: apzheng@163.com (A.P. Zheng).
Peer review under responsibility of Shenyang Pharmaceutical University.

https://doi.org/10.1016/j.ajps.2021.02.003

swallowing are still there [4]. Children are often referred to as "small adults", but in fact they are significantly different from adults physically and mentally. Paediatricians adjust the adult dose to children by relying on clinical experience, leading to the dosage description of “half tablets” often appears in prescriptions. To destroy the structure of the preparation may result in the pharmacokinetic change *in vivo* and bring potential toxicity and loss of efficacy [4–7]. It was reported that 75%–85% of adverse effects from drug therapy occurred as a result of inappropriate dosing or dose combinations [2]. A survey of the European Network on Drug Investigation in Children (ENDIC) revealed that ~50% of all prescriptions for hospitalized children in the EU were administered either in an off-label or an unlicensed manner [8,9]. In addition, children prefer to the medicine with adorable shape, bright color and sweet taste instead of the ordinary dosage forms [10–12]. Despite the significant advances in child preparations in recent years, the above issues remain as major challenges that the pharmaceutical technology currently has to face. Accompanied with the challenge, an opportunity to develop the innovative pharmaceutical manufacturing technology to achieve "tailor-made" preparations for children is arising.

3D printing (three-dimensional printing) technology has shown to be a promising approach to fabricate a personalized preparation [3,13,14]. 3D printing is also called "rapid prototyping", "solid free form fabrication" and "additive manufacturing" [1,15]. It is a technology based on digital models to construct objects through layer-by-layer printing and finally turns the blueprints on the computer into physical objects. 3D printing technology offers high flexibility through the controllable printing process to obtain products with various geometric shapes and functions. At present, 3D printing has been widely used in the construction industry, machinery industry, aerospace, medicine and other fields, in which great achievements have been made [16–18]. The first and only 3D printed drug - Spritam® (levetiracetam tablets, for suspension), a landmark in 3D printing technology of pharmaceutical research, was approved by FDA in 2015 [19]. Binder jet 3D printing (BJ-3DP) technology, also known as drop-on-powder (DoP) was applied to develop this formulation. Printing ink containing liquid binder and/or active pharmaceutical ingredient is loaded into the printing head and jetted on a powder bed in precise path and dose, and the printing processes will keep repeating to produce the desired 3D product layer-by-layer [20,21]. Compared with traditional tablets, Spritam® has a large drug loading capacity (~65%) and highly porous structure, which dramatically increases the surface area to allow the tablet to quickly dissolve in water [22,23].

The 3D printing techniques utilized in the pharmaceutical field are BJ-3DP, stereolithography (SLA) and fused deposition modeling (FDM). In the SLA process, the layered 3D structures are built by solidifying a thin layer of the liquid resin on the movable platform and curing the polymer with an ultraviolet (UV) laser beam across the liquid surface in a defined depth. The high accuracy and resolution properties of SLA makes it an attractive method for the fabrication of preparations with complex 3D internal structures. However, the application of SLA in the pharmaceutical industry is limited by the availability of biocompatible photopolymerizable oligomers [13]. Another disadvantage is that SLA uses mainly single materials, and the development of complex preparations such as polymer mixtures and drug-loaded structures is limited [1]. FDM is perhaps the most extensively investigated 3D printing technique in the pharmaceutical field. The flexibility of FDM allows it to manufacture drugs with different geometries or modify drug release behavior that can be used to personalize therapy [24]. However, the productivity of FDM is low and the thermal analysis of FDM preparations shows that high process temperatures lead to significant degradation of thermally unstable active pharmaceutical ingredientS (APIs) [25].

BJ-3DP is a simple, versatile, low-cost, high-speed process that provides a variety of possibilities for the fabrication of individual and customized preparations. It offers a wide range of starting materials (such as powder and binder solution) and is more widely applicable in pharmaceutical industry when compared with other 3D printing technologies (such as SLA and FDM) [22]. It is one of the most promising 3D printing techniques for the commercial production of pharmaceuticals up to now. Goole and Amighi provided an exhaustive literature overview of applied binders and solvents in DoP printing [13]. Infanger et al. used hydroxypropyl cellulose (HPC) as a solid binder for BJ-3DP with an ink consisting of ethanol and water, and acceptable tablets with high drug loading were obtained, demonstrating that HPC is a suitable solid binder for BJ-3DP to print robust dosage forms [20]. Wickström et al. prepared printable inks of the poorly water soluble drug indomethacin and fabricated printed drug delivery systems (DDS) in a flexible and personalized manner with improved dissolution properties using piezoelectric inkjet technology [14]. Inks containing drugs are also printed on hypromellose materials in the form of quick response codes, illustrating the ability of BJ-3DP to create functional labels and quality control measures [26,27]. Recent studies have also emphasized the ability of 3D printing to create lipid-based preparations (in particular, solid self-microemulsifying drug delivery systems (S-SMEDDS)) to improve the release of poorly soluble drugs [28–30]. However, BJ-3DP still faces some challenges, such as improper powder feeding and scraping, absence of the suitable ink, clogging of the nozzles, binder migration and bleeding [2,31]. The physicochemical properties of the final ink including surface tension and viscosity need to be controlled within a small region by combining the powder properties with the printing mechanism, and may result great change on the printability [20,32,33]. To control the printed object appearance precisely is difficult for BJ-3DP too, thus may lead to rough surface due to stacking of large-sized powder on top of each other. Even if more and more studies are focused on BJ-3DP, little consideration has been given to the feasibility of scale-up, and few products have been developed to meet the multiple needs of children, such as admirable appearance, flexible dose, immediate release characteristic, etc. [19–22].

In this study, an innovative color jet 3D printing (CJ-3DP) technology was developed to produce colorful cartoon tablets suitable for children, and the probability of scale-up was also evaluated. Compared with BJ-3DP, CJ-3DP can achieve a more exquisite appearance of the preparation through combining multiple printing heads loaded with different printing inks. This article conducts an exhaustive research on drug formulations, especially ink formulations, which plays crucial role in the feasibility and robustness of 3D printing. Compared

with ethanol, isopropanol has stronger prescription tolerance as a basic solvent in printing ink. To ensure that the quality of the product is not inferior to that of Spritam®, the determination of surface roughness, mechanical properties, microstructure and release characteristics of tablets was an important part of this study. Taking levetiracetam as a model drug, child-friendly cartoon CJ-3DP tablets with admirable appearances and immediate release characteristics were fabricated and characterized, which has great potential to be used as personalized preparation.

2. Materials and methods

2.1. Materials

Levetiracetam (>98%, Zhejiang Apeloa Jiayuan Pharmaceutical Co., Ltd., China) was used as API. Microcrystalline cellulose (MCC PH101, Asahi Kasei, Japan) was used as an excipient and disintegrant. Mannitol (PEARLITOL 50C, Roquette Freres, France) was used as a sweetener and excipient. Spearmint flavor (Kerry, Ireland) and sucralose (Alpha Hi-Tech, China) were used as flavouring agents. Colloidal silicone dioxide (Aerosil 200, Evonik Degussa GmbH, Germany) was used as glidant. Polyvinylpyrrolidone (PVP K30, BASF, Germany) (Mw $\sim 3.8 \times 10^4$) was used as printing ink binder. Glycerin was used as printing ink plasticiser, and polysorbate 20 was used as printing ink wetting agent. Spritam® (Aprecia Pharmaceuticals Company, USA). All pigments used were of food grade. All other reagents, such as ethanol and isopropanol, were of analytical grade.

2.2. Preparation of powder mixture and printing ink

Levetiracetam was crushed with a grinder (WF-150, Jiangyin Xinan Machinery Manufacturing Co., Ltd., China). MCC PH101, mannitol, sucralose and spearmint flavor were sifted through a 120-mesh sieve. Aerosil 200 sifted through a 40-mesh sieve was added to improve the fluidity of the powder. Blending of the above components was performed with a Hopper Mixer (HSD15, Canaan, China) at 20 rpm for 20 min to obtain the final powder mixture. The proportion of levetiracetam in the powder mixture was ~65%, so it is necessary to study the effect of its particle size. In this study, 50% (v/v) ethanol aqueous solution was used as the base solvent of the printing ink. To obtain stable droplet spraying and good adhesion effect with the powder, appropriate proportions of binder (PVP K30), plasticiser (glycerin) and wetting agent (polysorbate 20) were added into the base solvent, and a suitable ink was finally obtained. The color printing inks were obtained by adding edible water-soluble pigments.

2.3. Flow properties of the powder

A powder comprehensive characteristic tester (BT-1000, Bettersize, China) was used to determine the angle of repose ($n = 3$) and Hausner ratio ($n = 3$) of mixtures. The Hausner ratio can be calculated using measured values for bulk density (ρ_{bulk}) and tapped density (ρ_{tapped}) as follows (Eq. (1)) [34]:

$$\text{Hausner Ratio} = \rho_{tapped}/\rho_{bulk} \quad (1)$$

2.4. Particle size analysis of the powder

The particle size distribution was analysed by a laser diffractometer (HELOS, SYMPATEC GmbH, Germany) with a dry dispersion unit. Detection of the particles was carried out using the R5 lens with the detection range of 0.5–875 µm at a dispersion pressure of 5 bar ($n = 3$).

2.5. Surface tension and contact angle of the ink

The surface tension and contact angle were measured at 25 °C with a drop shape analyser (DSA25, Kruss GmbH, Germany) using the pendant drop method and sessile drop method, respectively ($n = 3$). The Young-Laplace equation and the circle fitting method were used to calculate the surface tension and the contact angle. In the process of measuring the contact angle, the powder was pressed into a 25 mm thin sheet using a tablet press under a pressure of 20 MPa to avoid the influence of the surface roughness.

2.6. Viscosity and density of the ink

The viscosity of the printing ink was measured at 25 °C with a viscometer (DV-III ULTRA, Brookfield, USA) in triplicate. 25 ml printing ink was added to a volumetric flask on a mass balance at 25 °C in triplicate, and the density of the printing ink was calculated by the ratio of mass to volume.

2.7. Printability

The printability of the ink can be evaluated with the inverse (Z) of the Ohnesorge number (Oh), which is related to the surface tension (γ), viscosity (η), density (ρ) and droplet diameter (a) of the printing ink (Eq. (2)). The equation takes into account the characteristics of the printing ink, and successful jetting of the printing ink can be achieved when the Z value is among 1–10 [26,35–37]. Studies have found that in low-viscosity fluids, satellite droplets are often formed when $Z > 10$, which leads to reduced printing resolution and precision [38,39]. However, when $Z < 14$, the satellite droplet can merge with the primary droplet before deposition without affecting the printing performance [19,39].

$$Z = 1/Oh = \sqrt{(\gamma \rho a)}/\eta \quad (2)$$

2.8. Dosage form design

The computer-aided design software 3D Sprint (3D systems, USA) was used to create colorful cartoon models with different appearances for children, such as a heart, candy, cartoon, etc. (Fig. 1), which would be more convenient for children to take. Based on the flexibility and accuracy of the 3D printing technology, the tablet strengths (adjusted by the tablet size) and internal spatial structures (*e.g.*, solid structure, hollow structure, hollow structure with internal support, lattice structure, etc.) can be adjusted to achieve a specific dosage and release behavior. Furthermore, the shape and color of the tablets can be changed according to the preferences of children.

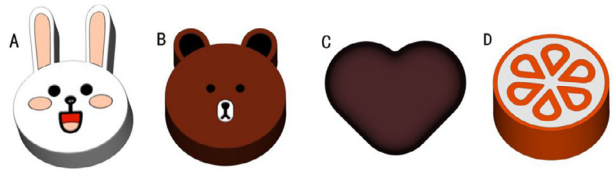

Fig. 1 – Schematic illustration of the colorful cartoon models, which can be changed according to preferences of children to improve their medication compliance. (A): Rabbit; (B): Bear; (C): Heart; (D): Candy.

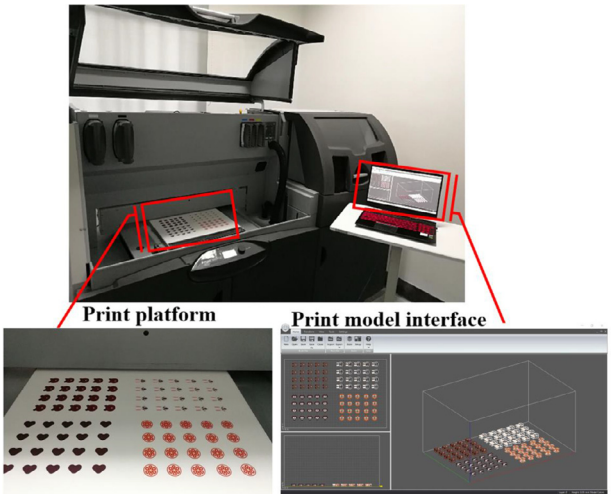

Fig. 2 – Schematic diagram of the printing process of colorful cartoon tablets using a binder jet 3D Printer.

2.9. *Printing process*

Printing was conducted using a binder jet 3D Printer (Projet CJP 660 Pro, 3D systems, USA). As shown in Fig. 2, the designed model file was uploaded to the software of the 3D printer, which sliced the model and sent the slices to the 3D printer. Thin layers of powder mixture (100 μm per layer) were spread across the platform. The print carriage moved across each layer, using 5 hot-bubble printing heads (HP11, Japan) to selectively deposit clear or colored printing inks of specific composition, which were loaded into a cartridge through a 10 μm filter. Each printing head has 304 nozzles, and a single droplet from the nozzle is 18 pl. The ink solidified the powder only in the cross-section of the designed model, and the remaining powder was used for support. The print resolution was 600 × 540 Dots Per Inch (DPI), and the maximum vertical build speed was 28 mm per hour. After printing, the tablets were dried at 40 °C for at least 1.5 h to remove organic solvent and excess moisture, and the support powder was recycled for reuse through an integrated vacuum system. The tablets were then cleaned with an air brush to remove excess powder.

2.10. *Physical properties of the tablet*

2.10.1. *Appearance and surface roughness*

The surface of the tablet should be visually intact and smooth. A three-dimensional white-light interference profilometer (Nexview, ZYGO, USA) was used to measure the surface roughness of the tablets. The tablets were observed at magnifications of 2.75 × with an objective lens and 1 × with an eyepiece to evaluate the characteristic surface roughness parameters, such as the root mean square height (Sq), arithmetic mean height (Sa) and maximum height (Sz). Sz is the sum of maximum peak height (Sp) and maximum valley depth (Sv).

2.10.2. *Hardness and friability*

The hardness and friability of the tablets were analysed using a friability and hardness tester (CJY-2C, Shanghai Huanghai Instruments Co., Ltd., China). The hardness (breaking force) of 6 tablets was measured by a fracture test, and the load at fracture was measured in Newtons (N). The friability of tablets was analysed in terms of their resistance to breaking. A minimum of 10 tablets (at least 6.5 g) were dusted, weighed and placed in the tester, which rotated at 25 rpm for 4 min. All powder was removed from the tablets, and they were weighed again to calculate the relative weight loss.

2.11. *Tablet microstructure*

2.11.1. *Scanning electron microscopy (SEM)*

The morphology of the printed tablets was investigated with SEM (JSM-7900F, JEOL, Japan) equipped with an electron optical instrument. A vacuum evaporator was used to spray a conductive layer on the surface of the sample. The acceleration voltage was then adjusted to 3.0 kV, and the samples were observed at magnifications of 50 × and 300 × .

2.11.2. *Porosity*

The pore size distribution and average pore diameter of the tablets were measured by a surface area and pore size analyser (AutoPore 9520, Micromeritics, USA), and the bulk density and apparent (skeletal) density were measured at 0.21 psia and 29,996 psia, respectively. The porosity can be calculated as follows: Porosity (%) = (1-bulk density/apparent (skeletal) density) × 100%).

2.11.3. *Raman spectroscopy*

A Thermo Fisher Scientific FT-Raman DXR2xi spectrometer was used to investigate the distribution of the components and the crystal form of levetiracetam in the 3D printed tablets. Regions of 1000 μm × 1000 μm and 300 μm × 300 μm were captured for Raman image acquisition and analysis, respectively, and the spectra were acquired using a 532 nm laser.

2.12. *Dispersible uniformity and in vitro drug release*

The dispersible uniformity was measured with a disintegration tester (ZB-1D, Tianda Tianfa Technology Co., Ltd., China) to determine the dispersion time of the tablets. The inner diameter of the stainless steel wire mesh of the measuring device was 710 μm. Dispersion time for 6 tablets was measured in purified water at 15–25 °C (usually 20 °C), and the maximum value was adopted. *In vitro* drug release was determined in a USP II paddle apparatus (RC806D, Tianda Tianfa Technology Co., Ltd., China) in 900 ml phosphate buffer

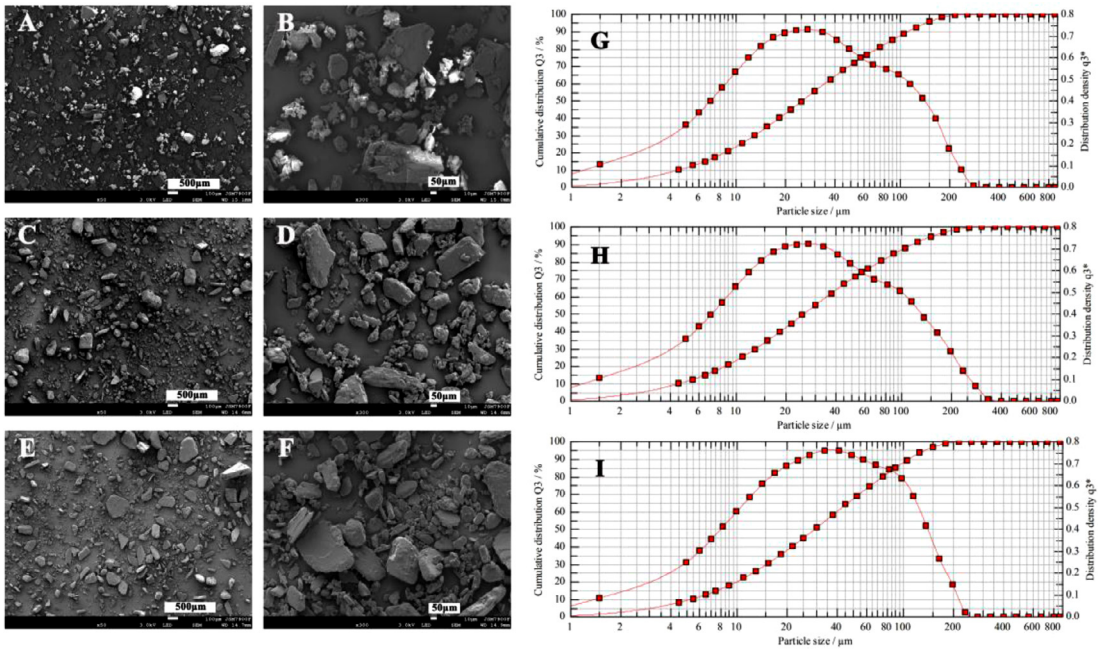

Fig. 3 – SEM images and particle size distribution diagrams of APIs crushed through different meshes. (A, B, G): Crushed through a 100 mesh; (C, D, H): Crushed through a 120 mesh; (E, F, I): Crushed through a 150 mesh.

solution (pH 6.8) at 37 °C with a paddle speed of 50 rpm. The release of 6 tablets was measured after 2.5, 5, 10, 15, 20 and 30 min and analysed using high-performance liquid chromatography (HPLC).

2.13. *Prediction of oral disintegration time*

A texture analyser (TA touch, BosinTech, China) was used to predict the oral disintegration time of the tablets with different internal spatial structures. In the experiment, a constant pressure test was employed, and the disintegration curve of the samples within 50 sec in 3 ml purified water was measured. The parameters were as follows, the pretest speed 5 mm/*sec*, the test speed 8 mm/*sec*, the trigger force 5 gf and the target pressure 50 gf (1 gf ≈ 0.0098 N).

2.14. *X-ray diffraction*

X-ray diffraction patterns of API, excipients and tablets were obtained with an X-ray diffractometer (D8 advance, Bruker, Germany) to confirm whether the crystal form of the API in the tablet changed. The scanning range was 3–40° with a step size of 0.02°, and the scanning speed was 0.02 sec per step with the Cu tube set to 40 kV and 40 mA.

3. Results and discussion

3.1. *Formulation development*

3.1.1. *Powder formulation*

Powder wettability and fluidity play vital role in CJ-3DP, especially in the control of the printing accuracy and uniformity, which mainly depend on the solubility and surface

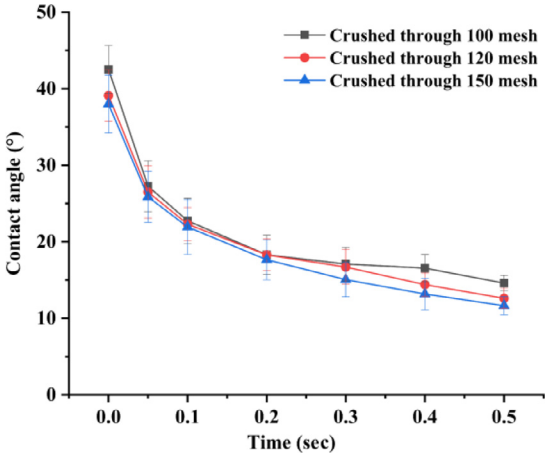

Fig. 4 – Contact angle of APIs crushed through different meshes and printing ink in a 40% (v/v) isopropanol aqueous solution containing 0.1% (w/w) PVP and 4% (w/w) glycerin over a time period of 0.5 sec.

morphology and particle size of the powder. In this study, levetiracetam was used as a model drug with a loading of ~65%, which is very soluble in water (1.04 g/ml) and freely soluble in ethanol (0.165 g/ml). As shown in Fig. 3 and 4, the surface morphology, particle size (D90 ≈ 120 μm, D50 ≈ 25 μm) and the wettability (all contact angle after 0.5 sec were below 15°) of the API have no significant change with various meshes, indicating that the API brittleness but not the mesh size played vital role in the crush process. Taken together, the API was determined to be crushed through a 120 mesh. Moreover, this study found that even if a small amount of particles were slightly larger than the thickness of the powder

Table 1 – Effect of Aerosil 200 in the powder mixture on the fluidity.

Proportion of Aerosil 200 in the powder mixture (w/w)	0	0.1%	0.2%	0.3%	0.5%
Repose angle (°)	47.74±2.79	44.11±2.01	42.03±1.42	40.80±1.15	38.36±1.63
Bulk density (g/cm^3)	0.38±0.01	0.41±0.01	0.46±0.01	0.48±0.02	0.49±0.01
Tapped density (g/cm^3)	0.68±0.01	0.68±0.01	0.68±0.01	0.70±0.01	0.70±0.01
Hausner ratio	1.79±0.04	1.67±0.04	1.48±0.03	1.45±0.04	1.41±0.02

layer (the particle size of some APIs was 20 μm larger than the layer thickness), no negative effects could be observed. This might be due to residual ink in the preceding layers that might deform plastically upon creation of a new layer and the larger particles were embedded in the powder bed through the movement of the roller [20].

To further improve the fluidity of the powder mixture, Aerosil 200 was added to the powder (as shown in Table 1). However, it was found that extra Aerosil 200 (>0.3%, w/w) led to excessive fluidity (the repose angle<40.80 ± 1.35, and the Hausner ratio<1.41 ± 0.02), resulting in substantial powder leakage from the hopper during the printing process and potential interlayer displacement caused by lack of friction between the particles. In fact, a repose angle of the mixed powder of 42.03° and a Hausner ratio of 1.48 could meet the requirements of 3D printing in terms of the powder fluidity, which was different from the requirement of traditional solid preparation (Hausner ratio below 1.34 is acceptable) [34]. Therefore, as shown in Table 1, the proportion of Aerosil 200 in the powder was determined to be 0.2%.

3.1.2. *Ink formulation*

In general, the greatest challenge in most inkjet processes is the development of the ink [20]. The printing ink needs appropriate viscosity, surface tension and wettability to meet the requirements of printability [32,33]. In this study, since levetiracetam is a water-soluble drug and accounts for a large proportion, water can be used as the basic solvent. However, considering the large surface tension (72 mN/m, 25 °C) and the slow volatilizing rate of water, it is usually used in conjunction with ethanol as the basic solvent. Previous study has mentioned that it is impossible to print when the concentration of ethanol is below 70% [20]. However, our study revealed that the printability of the ink is related to the jetting mechanism of the printing head and the properties of the powder. In this study, 50% (v/v) ethanol-water solution was initially used as the basic solvent, while poor jetting uniformity and interlaminar fracture occurred during scale-up process (Fig. 5A). It may be related to poor match of the ink with the printing head. When the organic solvent was below 37% (v/v), humps appeared during printing and resulted in rough surface of the tablets (Fig. 5B), while 40% (v/v) ethanol would give rise to interlaminar fracture. Regular and intact tablets were acquired when the organic solvent changed from ethanol to 40% (v/v) isopropanol (Fig. 5C). The reason may attribute to the boiling points of isopropanol and ethanol, which are 82 °C and 78 °C, respectively. Isopropanol has a better thermal stability and can jet fluently from the hot-bubble printing head. Moreover, the viscosity of isopropanol (2.430 mPa·s, 20 °C) is higher than that of ethanol (1.074 mPa·s, 20 °C), thus it will not tend to generate excessive penetration during the initial printing stage but keep good inkjet fluency and printing stability. It was further found that when isopropanol was below 35% (v/v), humps appeared again (similar to Fig. 5B), and when the isopropanol proportion was higher than 50% (v/v), a slight interlaminar fracture occurred (similar to Fig. 5A). Therefore, 40% (v/v) isopropanol aqueous solution was chosen as the basic solvent in the printing ink. This is the first study to use isopropanol as the basic solvent for CJ-3DP and achieve excellent printing results.

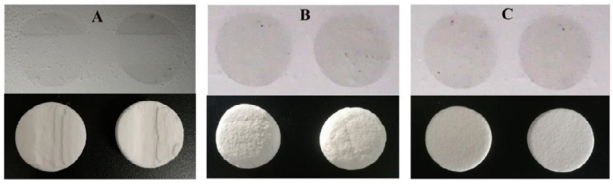

Fig. 5 – Effect of different organic solvents in printing inks on printability during scale-up process. (A): 50% (v/v) ethanol aqueous solution, poor jetting uniformity in the printing process and interlaminar fracture of the tablets; (B): 37% (v/v) ethanol aqueous solution, slow volatilization and rapid infiltration of the droplets result in rough bottom of the tablet; (C): 40% (v/v) isopropanol aqueous solution, good inkjet fluency and printing stability result in regular and intact tablets.

Adding PVP to the printing ink can usually improve the mechanical properties of the tablets. The results showed that the addition of PVP to the printing ink did not increase the tablet hardness but significantly reduced the tablet friability. The effects of different PVP proportions on the physicochemical properties of the printing ink and the critical quality attributes (CQAs) of the tablets are shown in Fig. 6A and 6B. The density and viscosity of the printing ink increased with PVP increasing, but the surface tension stayed constant. When the proportion of PVP in the ink was below 0.1% (w/w), the hardness of the tablets changed little with PVP increasing, but the friability decreased from 10.70% to 5.88%. However, excessive PVP (more than 0.5%, w/w) not only resulted in greater friability but also significantly increased the dispersion time, and the tablets could not be printed when the PVP proportion was 1%, which was related to the unstable jet due to the excessive viscosity of the printing ink. Although the optimized friability was higher than that of the tablets prepared in traditional way, it was similar to that of Spritam®. These results also showed that special attention needs to be paid in the packaging of immediate-release formulations prepared by CJ-3DP.

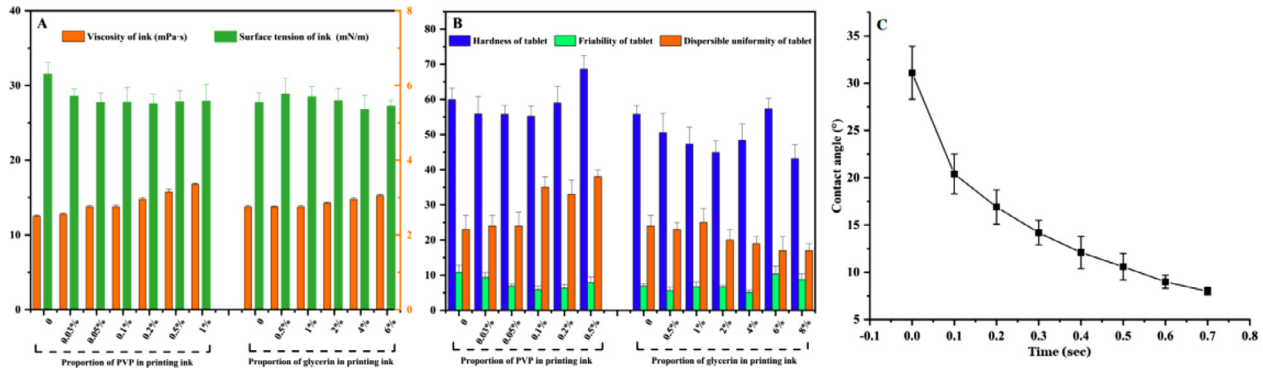

Fig. 6 – Effects of different PVP and glycerin proportions on the physicochemical properties of the printing ink and the critical quality attributes (CQAs) of the printed tablets. (A): The physicochemical properties of the printing ink; (B): The CQAs of the printed tablets; (C) Dynamic diagram of the contact angles of the determined printing ink with the powder.

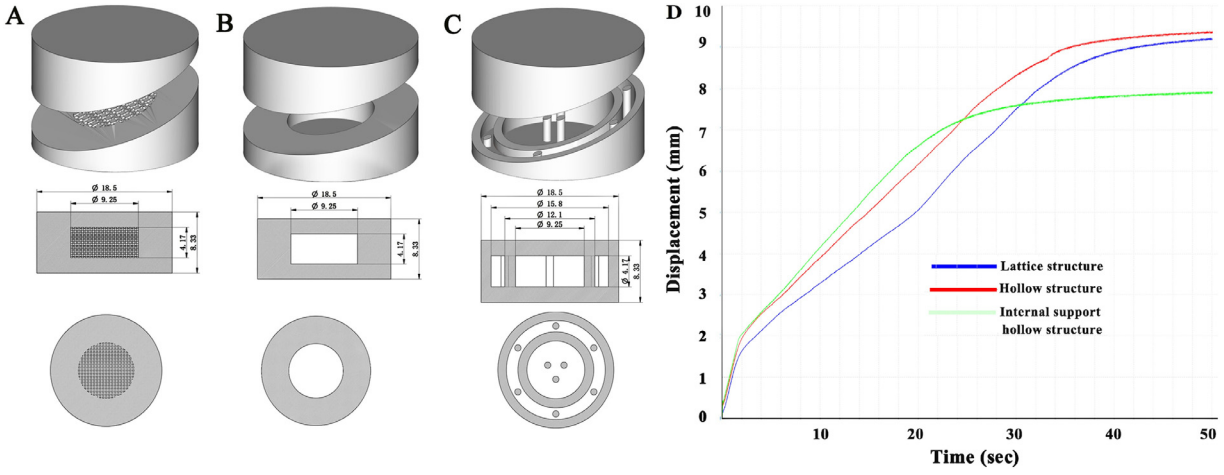

Fig. 7 – Schematic illustration of the different internal spatial structure models, which were designed to achieve faster disintegration and maintain the mechanical strength of the tablets. (A): Lattice structure; (B): Hollow structure; (C): Hollow structure with internal support; (D) Disintegration curve of the tablets with different internal spatial structures determined by a texture analyser at a constant pressure.

Recent studies have shown the benefits of glycerin application in 3D printing formulations [14,26,40,41]. Fig. 6A and 6B showed that the addition of glycerin to the printing ink at proportions within 4% (w/w) could significantly improve the formability of the tablets and accelerate the dispersion. However, a higher glycerin content also reduces the mechanical properties and increases the surface roughness of the tablets, which may be related to the excessive viscosity and poor jetting uniformity. Theoretically, polysorbate as a surfactant can significantly improve the wettability of the printing ink, but no obvious improvement was observed in this study, which may be related to the good wettability of the printing ink itself [26].

The final determined printing ink consisted of 40% (v/v) isopropanol aqueous solution containing 0.05% (w/w) PVP and 4% (w/w) glycerin and has a density (ρ) of 0.9469 ± 0.0004 g/cm^3, a viscosity (η) of 3.55 ± 0.03 mPa•s, and a surface tension (γ) of 26.50 ± 1.08 mN/m. The resulted Z value of the ink is 7.73, which could meet the requirements in the range of 1 to 14. The contact angle results of this printing ink were shown in Fig. 6D and confirmed the good wettability of the printing ink with the powder.

3.2. *Design of the spatial structure model*

To further accelerate drug release, three types of internal spatial structure models, lattice structure, hollow structure and hollow structure with internal support, were designed as shown in Fig. 7A-7C. The shell thickness of the lattice structure and the hollow structure model was 1/4 of the tablet size. On the basis of the hollow structure model, the 9 columns in the shell and the hollow part uniformly distributed throughout the whole structure to achieve faster disintegration and maintain the mechanical properties of the tablets. According to the results, the average hardness was only 13 N, indicating that the mechanical properties of the hollow structure with the internal support tablet was poor, and the tablet failed the friability test. The average hardness of the hollow structure and lattice structure tablet were 61 and 59 N, respectively, and the tablet remained intact after the friability test. In terms of

Fig. 8 – 3D printed cartoon tablets with different strengths. (A): 1000 mg strength; (B): 250 mg strength.

the disintegration curve determined by the texture analyser at a constant pressure shown in Fig. 7D, the hollow structure tablet showed a faster disintegration time and its mechanical properties were similar to the lattice structure, so the hollow structure was chosen as the tablet model.

3.3. *Cartoon tablets*

Cartoon tablets based on hollow structure with different strengths (1000 mg and 250 mg) and appearences were designed by 3D Sprint. To minimize the use of pigment, color printing inks were used only when printing the outer layer of the tablet, and transparent printing ink was used to print the inner layer of the tablet except for the hollow part. As shown in Fig. 8, cartoon tablets were printed with high accuracy and reproducibility without any defects, which could improve the drug compliance of children. In general, complex shape tablets have poor mechanical properties due to irregular movement. Surprisingly, the cartoon tablets showed good hardness (21.05- 59.21 N), friability (2.77%–5.75%) and dispersion uniformity (9–17 sec) (Fig. 9), except for 250 mg rabbit-shaped tablets failed the friability test (partial breakage of the ear). It was attributed to the poor mechanical properties of long ears, suggesting that excessively irregular shapes 0.02 s should be avoided in the design of cartoon tablet models, such as cartoon models with long and thin protruding parts.

The results of the *in vitro* drug release profiles in Fig. 10 showed that all of the cartoon tablets with 1000 mg strength showed rapid release characteristics, and the drug was almost completely released after 2.5 min. Both of the above results of the cartoon tablets(except for 250 mg rabbit-shaped tablets) were similar to those of Spritam®. Moreover, the appearance did not obviously affect the mechanical properties or the release of the tablets. See appendix 1 for an immediate dispersion video of different cartoon tablets in room temperature water.

3.4. *Dosage model*

3D printing technology allows for a flexible adjustment of the drug dose through the design of model size for personalized drug administration. However, for successful preparation of

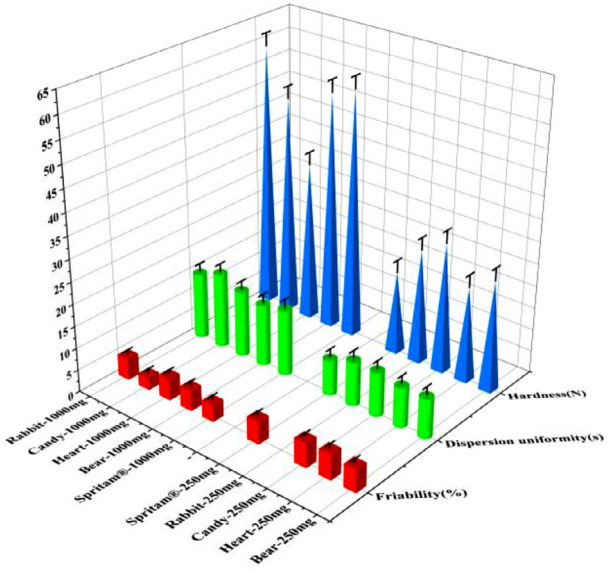

Fig. 9 – Friability, hardness and dispersion uniformity of 3D printed cartoon tablets with different strengths and Spritam® with the corresponding strengths.

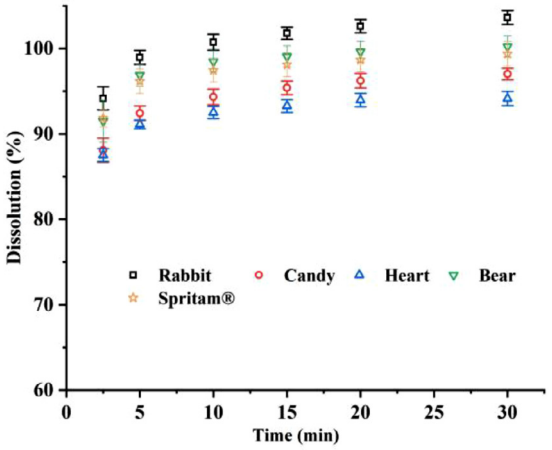

Fig. 10 – *In vitro* drug release profiles of 3D printed cartoon tablets (1000 mg strength) and Spritam® (1000 mg strength) at pH 6.8 ($n = 6$).

tablets with different model sizes, the printing ink, powder and printing parameters need to cooperate with each other to achieve the requirement of precision printing. In this study, 3D Sprint software was used to design tablet models of different sizes, and the theoretical strengths were 160 mg, 250 mg, 500 mg, 750 mg and 1000 mg. A schematic diagram of the corresponding dosage model is shown in Fig. 11A-C. The diameter and height of the tablets are proportional. Hollow model tablets of different sizes were printed with the defined printing ink and powder, and the weight and content (used to calculate strength) of each tablet were determined. With the tablet model volume as the X axis and the tablet specification as the Y axis, a correlation between model size and dose was established. There was a good

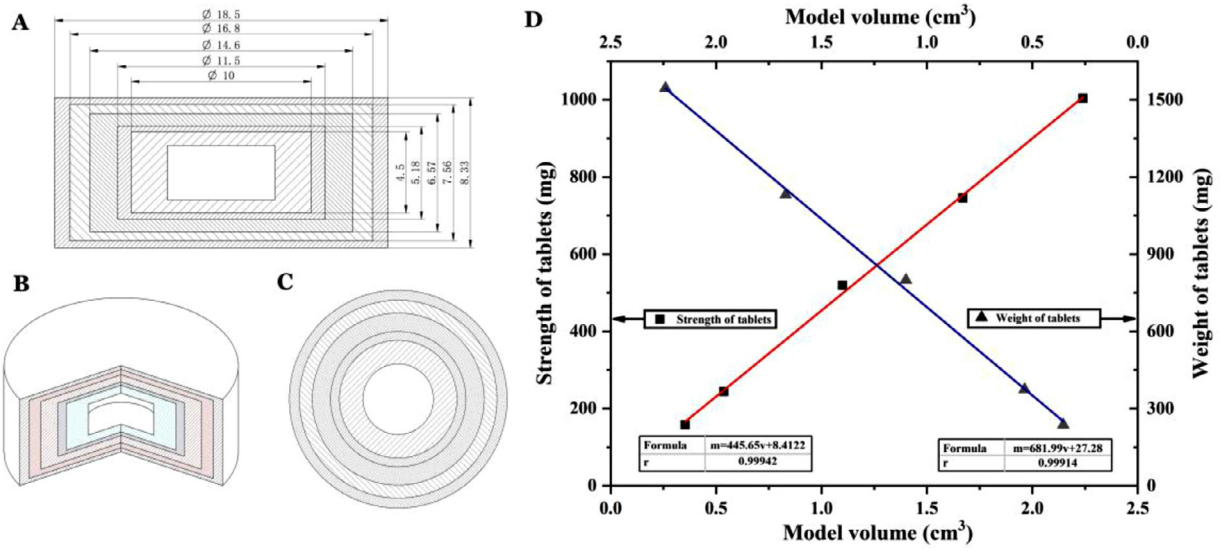

Fig. 11 – Schematic diagram of different size models for adjusting the drug dose. (A): Side-view dimension profile; (B): Three-dimensional profile; (C): Top view; (D) Individual dosage model of the model volume (v) and the tablet weight (m_1) and strength (m_2), which can be used to flexibly adjust the drug dose.

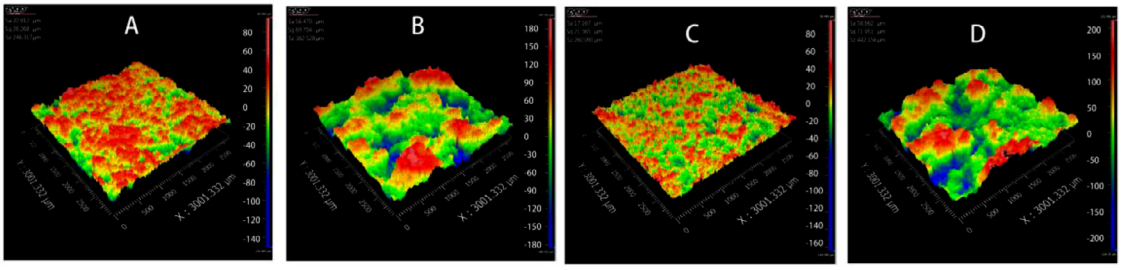

Fig. 12 – 3D topography of 3D printed tablets with different strengths ((A): Sample 1000 mg, (C): Sample 250 mg) and Spritam® with the corresponding strengths ((B): Spritam® 1000 mg, (D): Spritam® 250 mg).

linear relationship between the model volume (v) and the tablet weight (m_1) and strength (m_2) (Fig. 11D), which can be described by the following formulas: $m_1 = 681.99v + 27.28$ ($r = 0.9991$), $m_2 = 445.65v + 8.4122$ ($r = 0.9994$). It has been proven that the drug dose can be flexibly adjusted by the size of the model design without an additional mold.

3.5. *Surface roughness*

The surface roughness of 3D printed tablets with different strengths was observed using a three-dimensional white-light interference profilometer and compared with Spritam®. As shown in Fig. 12 and 13, the typical surface roughness values of 250 mg and 1000 mg samples were 21.365 and 26.268 μm, respectively; the corresponding Sq values of Spritam® were 69.704 and 71.951 μm, respectively. As apparent from the 3D topography and surface roughness characteristic parameters, such as Sq, Sa and Sz, the surfaces of the tablets with strengths as both 250 mg and 1000 mg were smoother than those of Spritam®. The appropriate viscosity of the printing ink and particle size of the powder provide the probability of accompanying the smooth surface of the tablets.

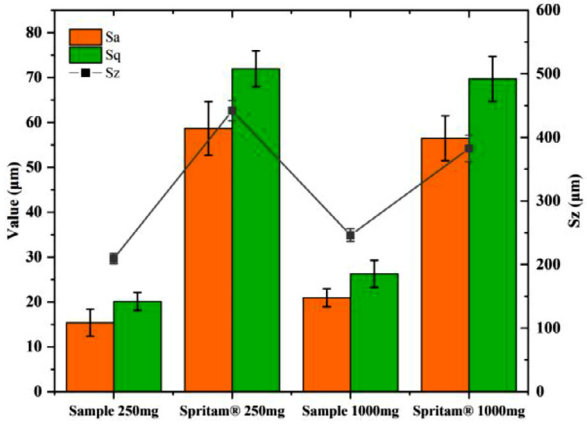

Fig. 13 – Typical values of surface roughness of 3D printed tablets with different strengths and Spritam® with the corresponding strengths.

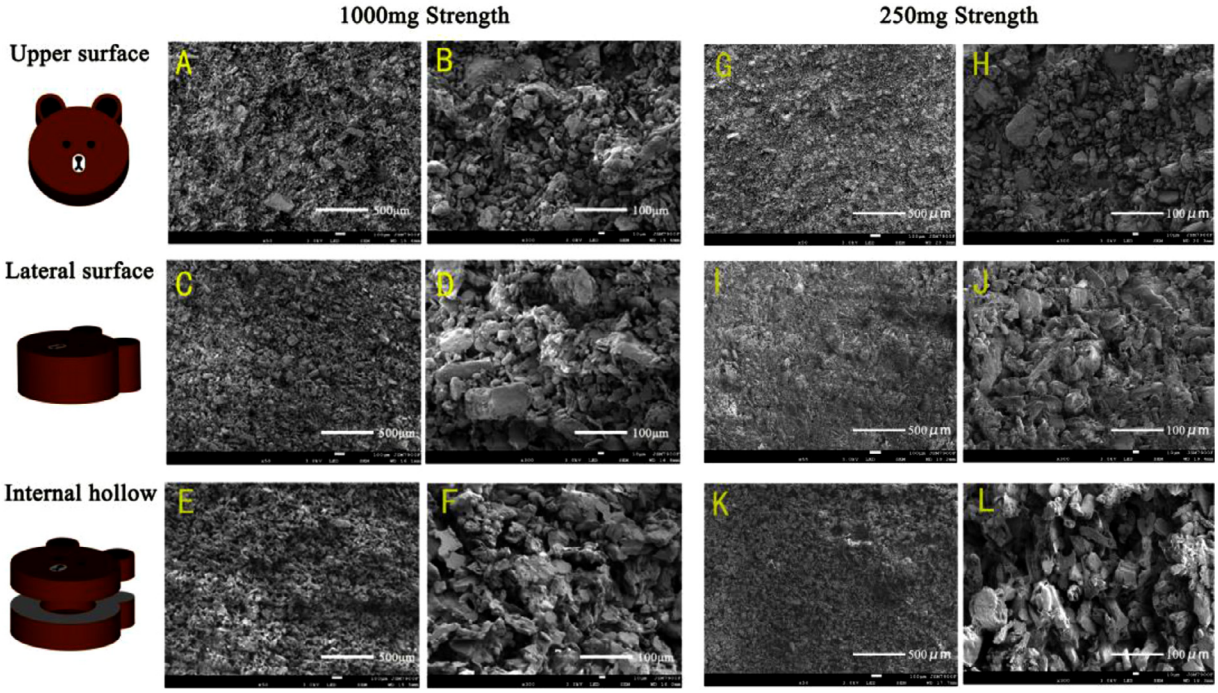

Fig. 14 – SEM images of 3D printed tablets with 1000 mg strength (A-F) and 250 mg strength (G-L). (A, G): upper surface (50 ×); (B, H): upper surface (300 ×); (C, I): Lateral surface (50 ×); (D, J): Lateral surface (300 ×); (E, K): Internal hollow (50 ×); (F, L): Internal hollow (300 ×).

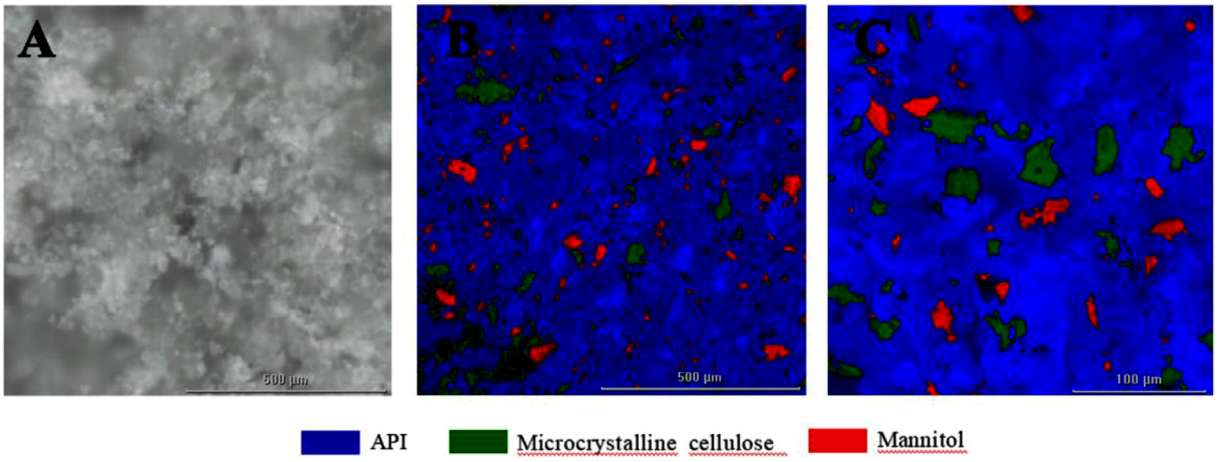

Fig. 15 – Micro-Raman image of 3D printed tablets with 1000 mg strength(A: Microscopic image; B: Raman image in the region of 1000 μm x 1000 μm; C: Raman image in the region of 300 μm x 300 μm).

3.6. *Tablet microstructure*

Fig. 14 showed the microstructures of 3D printed tablets with different strengths observed by SEM at magnifications of 50 × and 300 × . Many pores were distributed on the upper surface (Fig. 14A and 14G, 50 ×) and the lateral surface (Fig. 14C and 14I, 50 ×) of the tablet. Meanwhile, according to the more microscopic SEM (Fig. 14B, 14D, 14H and 14J, 300 ×), the particles appeared to be bound together, and the structure of the tablet shell was relatively tight. This structural feature allows for improved appearance and mechanical properties and rapid water penetration.The SEM images (Fig. 14E&14 K, 50 × and Fig. 14F&14 L, 300 ×) revealed that the internal hollow region of the tablet was uniform powder without any bonding trace, and faster drug release can be achieved when water comes into contact with the powder. Fig. 15 is the micro-Raman images for the surface of the 3D printed tablet. The microscopic image (Fig. 15A) showed that the surface of the tablet was bonded by white crystals. The characteristic Raman spectra of the regions 1000 μm × 1000 μm (Fig. 15B) and 300 μm × 300 μm (Fig. 15C) showed that the microcrystalline cellulose in the green region and mannitol in the red region

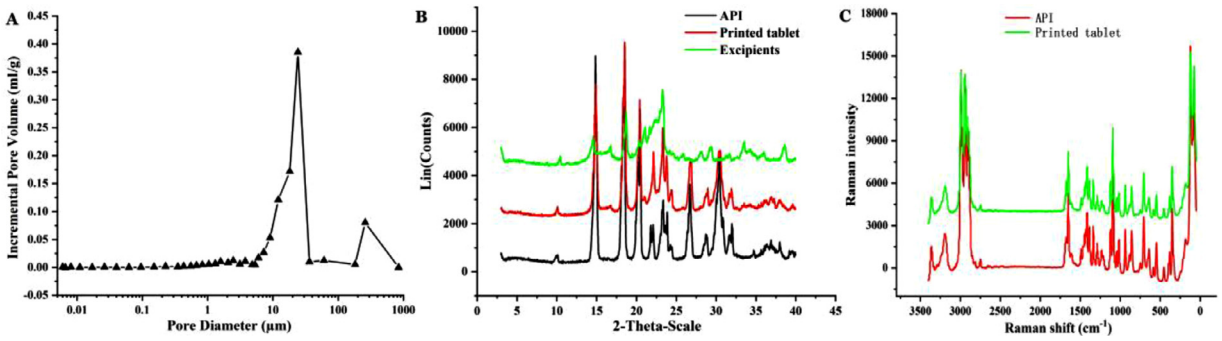

Fig. 16 – (A) Pore size distribution of 3D printed tablets with 1000 mg strength; (B) X-ray diffraction patterns of the API, excipients and the printed tablets; (C) Raman spectrograms of the API and the printed tablets.

were uniformly dispersed, and the API in the blue region was continuous and closely bonded. Thus, the above microscopic phenomenon suggested that the powder was mainly bonded by levetiracetam in the process of layer-by-layer printing. This was related to the good wettability of levetiracetam as previous result (Fig. 4) and the formation of solid bridge after printing and drying.

The porosity of the 3D printed tablets was as high as 55.6%. Fig. 16A showed the pore size distribution of the tablets, most of which were tiny with an average pore size of 3.16 μm and a total pore area of 1.23 m^2/g. Compared with Spritam® (58.1% porosity with an average pore size of 6.65 μm and a total pore area of 0.64 m^2/g), the tablets printed in this study had a larger number and area of pores. It is further proven that the tablet had porous structures, and water can penetrate into these capillary channels to achieve the rapid dispersion of the tablet. This structural feature of the printed tablet was mainly attributed to the layer-by-layer approach of the CJ-3DP. Particle accumulation could be facilitated through bonding of the binder and the recrystallization of soluble excipients without plastic deformation. Thus, a large porosity could be achieved on the basis of ensuring the mechanical properties of the tablet. Simultaneously, the hollow model was used to achieve a larger porosity with the protection of the shell to achieve the rapid release of the drug.

3.7. *Crystal form*

X-ray diffraction patterns and Raman spectrograms are shown in Fig. 16B and C. The results showed that the crystal form of API in the tablet did not change, and it was still the crystal form I reported in the literature [42,43]. It has been proven that the crystal form of the API was stable during the printing process [44].

4. Conclusion

This study proves that the preparation of colorful cartoon levetiracetam pediatric tablets can be realized by using CJ-3DP. Through the optimization of formulation and tablet structure, the 3D printed tablets had a admirable appearance and a lower surface roughness, all of which were notably improved compared with the properties of Spritam®. Meanwhile, the 3D printed tablets had strong mechanical properties and immediate release characteristics. Compared with Spritam®, the total number and area of pores of the tablets printed in this study were significantly higher with the similar porosity. A large number of small holes formed easy-wetting capillary channels when the tablet was in contact with water, which could penetrate into the tablet through the capillary channels and wet the whole tablet quickly, resulting in its disintegration. Moreover, this study proves that the dispersion of tablets can be further accelerated by adjusting the internal spatial structure of the model, and the flexible adjustment of drug strengths can be achieved by establishing a dosage model to realize personalized administration.

The biggest challenge, for CJ-3DP and most inkjet processes in general, is the development of the ink. In this study, exhaustive experiments were carried out to determine the appropriate ink, and the applicability of the formulation to scale-up the production was considered. However, different powders and printing heads usually lead to different optimal compositions of the ink. From the view of scale-up production, when using hot-bubble printing heads, the proportion of organic solvent in the ink should not be too large to avoid interlaminar fracture of the tablets caused by poor jetting uniformity. Compared with the traditional preparation process, 60 min are required in CJ-3DP to print 120 tablets in this study. Although there is an immediate potential for unit dose fabrication with greatly reduced processing steps, the production efficiency is still low. The use of production printing equipment in the future is expected to increase the production efficiency, but 3D printing equipment still needs to be continuously improved to meet the requirements of high printing accuracy and efficiency. An interesting characteristic of this technology is that once a stable formulation and processing parameters are obtained, it can be scaled up for commercial production. In the foreseeable future, the development of 3D printing technology in personalized medical preparations for children deserves more attention.

Conflicts of interest

No potential conflict of interest was reported by the authors.

Acknowledgements

This work was supported by the National Natural Science Foundation of China (No. 82073793), the National Major Science and Technology Projects of China (No. 2018ZX09721003–007/ No. 2018ZX09J18107).

Author contributions

Zengming Wang: carried out the experiments and performed data analysis, wrote the paper; Xiaolu Han, Ruxin Chen, Jingru Li and Nan Liu: participated part of the experiments; Aiping Zheng, Jing Gao, Hui Zhang and Xiang Gao: designed the research and modified the paper.

Supplementary materials

Supplementary material associated with this article can be found, in the online version, at doi:10.1016/j.ajps.2021.02.003.

REFERENCES

[1] Palo M, Hollander J, Suominen J, Yliruusi J, Sandler N. 3D printed drug delivery devices: perspectives and technical challenges. Expert Rev Med Devices 2017;14(9):685–96.
[2] Alhnan MA, Okwuosa TC, Sadia M, Wan KW, Ahmed W, Arafat B. Emergence of 3D printed dosage forms: opportunities and challenges. Pharm Res 2016;33(8):1817–32.
[3] Afsana Jain V, Haider N, Jain K. 3D printing in personalized drug delivery. Curr Pharm Des 2018;24(42):5062–71.
[4] Trofimiuk M, Wasilewska K, Winnicka K. How to modify drug release in paediatric dosage forms? novel technologies and modern approaches with regard to children's population. Int J Mol Sci 2019;20(13):3200.
[5] Batchelor HK, Marriott JF. Formulations for children: problems and solutions. Br J Clin Pharmacol 2015;79(3):405–18.
[6] Lopez FL, Ernest TB, Tuleu C, Gul MO. Formulation approaches to pediatric oral drug delivery: benefits and limitations of current platforms. Expert Opin Drug Deliv 2015;12(11):1727–40.
[7] Richey RH, Shah UU, Peak M, Craig JV, Ford JL, Barker CE, et al. Manipulation of drugs to achieve the required dose is intrinsic to paediatric practice but is not supported by guidelines or evidence. BMC Pediatr 2013;13:81.
[8] Conroy S, Choonara I, Impicciatore P, Mohn A, Van Den Anker J. Survey of unlicensed and off label use in paediatric wards in european countries. european network for drug investigation in children. BMJ-Brit Med J 2000;320(7227):79–82.
[9] Breitkreutz J. European perspectives on pediatric formulations. Clin Ther 2008;30(11):2146–54.
[10] Preis M, Öblom H. 3D-printed drugs for children-are we ready yet. AAPS PharmSciTech 2017;18(2):303–8.
[11] Davies EH, Tuleu C. Medicines for children: a matter of taste. J Pediatr 2008;153(5):599–604 e2.
[12] Mennella JA, Beauchamp GK. Optimizing oral medications for children. Clin Ther 2008;30(11):2120–32.
[13] Goole J, Amighi K. 3D printing in pharmaceutics: a new tool for designing customized drug delivery systems. Int J Pharm 2016;499(1–2):376–94.
[14] Wickström H, Palo M, Rijckaert K, Kolakovic R, Nyman JO, Määttänen A, et al. Improvement of dissolution rate of indomethacin by inkjet printing. Eur J Pharm Sci 2015;75:91–100.
[15] Chhaya MP, Poh PS, Balmayor ER, van Griensven M, Schantz JT, Hutmacher DW. Additive manufacturing in biomedical sciences and the need for definitions and norms. Expert Rev Med Devices 2015;12(5):537–43.
[16] Jensen G, Morrill C, Huang Y. 3D tissue engineering, an emerging technique for pharmaceutical research. Acta Pharm Sin B 2018;8(5):756–66.
[17] Yang J, Liu X, Fu Y, Song Y. Recent advances of microneedles for biomedical applications: drug delivery and beyond. Acta Pharm Sin B 2019;9(3):469–83.
[18] Li C, Wang J, Wang Y, Gao H, Jin Y. Recent progress in drug delivery. Acta Pharm Sin B 2019;9(6):1145–62.
[19] Prasad LK, Smyth H. 3D Printing technologies for drug delivery: a review. Drug Dev Ind Pharm 2016;42(7):1019–31.
[20] Infanger S, Haemmerli A, Iliev S, Baier A, Stoyanov E, Quodbach J. Powder bed 3D-printing of highly loaded drug delivery devices with hydroxypropyl cellulose as solid binder. Int J Pharm 2019;555:198–206.
[21] Wilts EM, Ma D, Bai Y, Williams CB, Long TE. Comparison of linear and 4-arm star poly(vinyl pyrrolidone) for aqueous binder jetting additive manufacturing of personalized dosage tablets. ACS Appl Mater Interfaces 2019;11(27):23938–47.
[22] Shi K, Tan DK, Nokhodchi A, Maniruzzaman M. Drop-on-powder 3D printing of tablets with an anti-cancer drug, 5-fluorouracil. Pharmaceutics 2019;11(4):150.
[23] Qi S, Craig D. Recent developments in micro- and nanofabrication techniques for the preparation of amorphous pharmaceutical dosage forms. Adv Drug Deliv Rev 2016;100:67–84.
[24] Skowyra J, Pietrzak K, Alhnan MA. Fabrication of extended-release patient-tailored prednisolone tablets via fused deposition modelling (FDM) 3D printing. Eur J Pharm Sci 2015;68:11–17.
[25] Sadia M, Sośnicka A, Arafat B, Isreb A, Ahmed W, Kelarakis A, Alhnan MA. Adaptation of pharmaceutical excipients to FDM 3D printing for the fabrication of patient-tailored immediate release tablets. Int J Pharm 2016;513(1–2):659–68.
[26] Cader HK, Rance GA, Alexander MR, Goncalves AD, Roberts CJ, Tuck CJ, et al. Water-based 3D inkjet printing of an oral pharmaceutical dosage form. Int J Pharm 2019;564:359–68.
[27] Edinger M, Bar-Shalom D, Sandler N, Rantanen J, Genina N. QR encoded smart oral dosage forms by inkjet printing. Int J Pharm 2018;536(1):138–45.
[28] Trenfield SJ, Awad A, Madla CM, Hatton GB, Firth J, Goyanes A, et al. Shaping the future: recent advances of 3D printing in drug delivery and healthcare. Expert Opin Drug Deliv 2019;16(10):1081–94.
[29] Vithani K, Goyanes A, Jannin V, Basit AW, Gaisford S, Boyd BJ. A proof of concept for 3D printing of solid lipid-based formulations of poorly water-soluble drugs to control formulation dispersion kinetics. Pharm Res 2019;36(7):102.
[30] Vithani K, Goyanes A, Jannin V, Basit AW, Gaisford S, Boyd BJ. An overview of 3D printing technologies for soft materials and potential opportunities for lipid-based drug delivery systems. Pharm Res 2018;36(1):4.
[31] Yu DG, Zhu LM, Branford-White CJ, Yang XL. Three-dimensional printing in pharmaceutics: promises and problems. J Pharm Sci 2008;97(9):3666–90.
[32] Buanz AB, Saunders MH, Basit AW, Gaisford S. Preparation of

personalized-dose salbutamol sulphate oral films with thermal ink-jet printing. Pharm Res 2011;28(10):2386–92.
[33] Kolakovic R, Viitala T, Ihalainen P, Genina N, Peltonen J, Sandler N. Printing technologies in fabrication of drug delivery systems. Expert Opin Drug Deliv 2013;10(12):1711–23.
[34] The united states pharmacopeial convention. Rockville: The United states pharmacopeia; 2019. USP43-NF38 p. 7993–5.
[35] Derby B. Inkjet printing of functional and structural materials: fluid property requirements, feature stability, and resolution. Annu Rev Mater Sci 2010;40(1):395–414.
[36] Fromm JE. Numerical calculation of the fluid dynamics of drop-on-demand jets. IBM J Res Dev 2010;28(3):322–33.
[37] Reis N, Derby B. Ink jet deposition of ceramic suspensions: modeling and experiments of droplet formation. Mrs Proc 2000;625:117–22.
[38] Martin GD, Hoath SD, Hutchings IM. Inkjet printing - the physics of manipulating liquid jets and drops. J Phys Conf Ser 2008;105(1):012001.
[39] Jang D, Kim D, Moon J. Influence of fluid physical properties on ink-jet printability. Langmuir 2009;25(5):2629–35.
[40] Zidan A, Alayoubi A, Coburn J, Asfari S, Ghammraoui B, Cruz CN, et al. Extrudability analysis of drug loaded pastes for 3D printing of modified release tablets. Int J Pharm 2019;554:292–301.
[41] Jacob J, Coyle N, West TG, Monkhouse DC, Surprenant HL, Jain NB. Rapid disperse dosage form containing levetiracetam. AUS 2018 2017202752[P].
[42] Parthasaradhi RB, Rathnakar RK, Raji RR, Muralidhara RD, Subash Chander RK. Novel crystalline forms of levetiracetam; 2005. USA, 2005143445[P].
[43] Herman C, Vermylen V, Norberg B, Wouters J, Leyssens T. The importance of screening solid-state phases of a racemic modification of a chiral drug: thermodynamic and structural characterization of solid-state phases of etiracetam. Acta Crystallogr 2013;69(Pt 4):371–8.
[44] Xu K, Xiong X, Guo L, Wang L, Li S, Tang P, et al. An investigation into the polymorphism and crystallization of levetiracetam and the stability of its solid form. J Pharm Sci 2015;104(12):4123–31.